

Y. Saito

PROCEEDINGS

PART 2.

INTERNATIONAL CONFERENCE ON ELECTRICAL MACHINES

LAUSANNE, SWITZERLAND

18-21 September 1984

Organized by the
Swiss Federal Institutes of Technology
Lausanne and Zürich

CALCULATIONS ON THE TEMPERATURE DISTRIBUTION OF DC-MACHINE ARMATURE
BY FINITE ELEMENT METHOD

T. YAMAMURA, Y. SAITO and H. NAKAMURA

College of Engineering, Hosei University, JAPAN

INTRODUCTION

Of all types of electric motors the DC-motor is by far the most versatility used in machines, because such as its wide range adjustable motor speed and constant mechanical power output or torque characteristics.

In the design of DC machines, the estimation of the temperature rise in the armature is now becoming to one of the most serious problems for modern compact high power DC motors. In spite of the various methods proposed for calculating the temperature rise in the armature, very few have been used in the practical design. Since it was difficult to treat the local heating problems based on the conventional means of treating an armature as a single body, a method based on the thermal equivalent method had been proposed by Yamamura for JNR traction motors[1,2], and it had been reported that this method was quite effectively used for the other types of DC machines[3,4,5].

In this paper, an initial experiment based on finite element methods(FEM) for the estimation of temperature distribution in the DC machine armature is carried out. Because of the difficulty of taking into account the forced cooling conditions, only the limited cases have been analyzed by FEM(e.g. Ref. [6]). In order to overcome this difficulty, we propose a modified finite element method that combines the conventional FEM with the experimental formulae for forced cooling condition. Some examples of calculated results are given and compared with those of the experimental results. As a result, it is revealed that our approach is one of the methods of introducing the forced cooling condition in the DC machine armature to FEM.

FORMULATION OF FUNCTIONALS

The estimation of temperature distribution is reduced to solve the following partial differential equation:

$$\nabla \cdot (\lambda \nabla \phi) = -f, \quad (1)$$

where λ , ϕ and f are the thermal conductivity, thermal (scalar) potential function and heat source, respectively. The formal functional of Eq. (1) is given by

$$F = \int_V \left\{ \frac{\lambda}{2} |\nabla \phi|^2 - f\phi \right\} dv + \int_S \phi \left(\frac{\partial \phi}{\partial n} \right) ds, \quad (2)$$

where $\partial \phi / \partial n$ denotes the normal derivative to the boundary direction. When we consider the region shown in Fig. 1, then the term related to the boundary in Eq. (2) is reduced to zero in the region not interfacing to the forced cooling boundary in Fig. 1 [6]. Namely, Eq. (2) reduces to

$$F = \int_V \left\{ \left(\frac{\lambda}{2} \right) |\nabla \phi|^2 - f\phi \right\} dv, \quad (3)$$

in the interior region of Fig. 1. However, in the region interfacing the forced cooling boundary in Fig. 1, it is obvious that the homogenous Neumann condition is not automatically satisfied in the functional minimization process. Thus, it must be taken some means for the surface integral term (second term of the right-side in Eq. (2)).

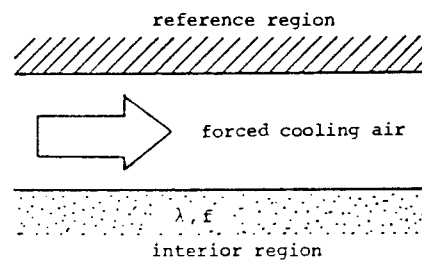


Fig. 1. An illustrative example of the forced cooling air boundary problem.

In fact, when we neglect this boundary condition, the finite element implementation based on only Eq. (3) yields poor results. Yamamura and Yamazaki have derived the experimental formulae of surface heat transfer by forced cooling effect in JNR traction motors [7,8]. Their formulae are generally expressed as

$$\alpha = \alpha (u_i, N, a, b, c), \tag{4}$$

where u_i and N are the axial velocity of the cooling air at each region and rotating speed of the armature, respectively. The other parameters a, b, c in Eq. (4) depend on the mechanical dimensions of each region. By means of Eq. (4), it is assumed that the term related to the forced cooling boundary in Eq. (2) is modified to

$$\int_s \phi (\partial\phi/\partial n) ds = (\phi_d^2/2) \int_s \alpha ds, \tag{5}$$

where ϕ_d is the potential difference between the reference point and surface. Thus, the functional containing the forced boundary region is reduced to

$$F = \int_v \{ (\lambda/2) |\nabla\phi|^2 - f\phi \} dv + (\phi_d^2/2) \int_s \alpha ds. \tag{6}$$

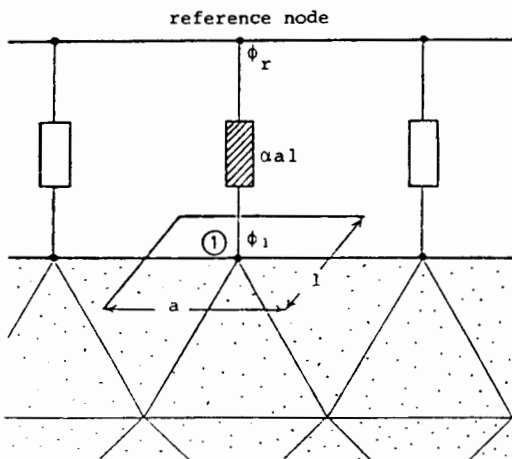


Fig. 2. Mesh systems of Fig. 1.

FINITE ELEMENT DISCRETIZATION

For simplicity, we discretize the regions shown in Fig. 1 by using the first order triangular finite element. The minimization of functional makes the regions in Fig. 1 into the mesh network system as shown in Fig. 2. As shown in Fig. 2, the surface integral term in Eq. (6) yields the elements between the boundary and reference nodes. When we consider the node 1 in Fig. 2, the surface integral of Eq. (6) is performed as

$$F_b = (\phi_d^2/2) \int_s \alpha ds = \{ (\phi_1 - \phi_r)^2 / 2 \} \alpha a l, \tag{7}$$

where a, l, ϕ_1 and ϕ_r are shown in Fig. 2. The minimization of Eq. (7) yields

$$\partial F_b / \partial \phi_1 = (\phi_1 - \phi_r) \alpha a l. \tag{8}$$

According to Eq. (8), the element between the node 1 and reference node in Fig. 2 is given as $\alpha a l$. The other elements related to the boundary nodes are given in much the same procedure as Eqs. (7) and (8).

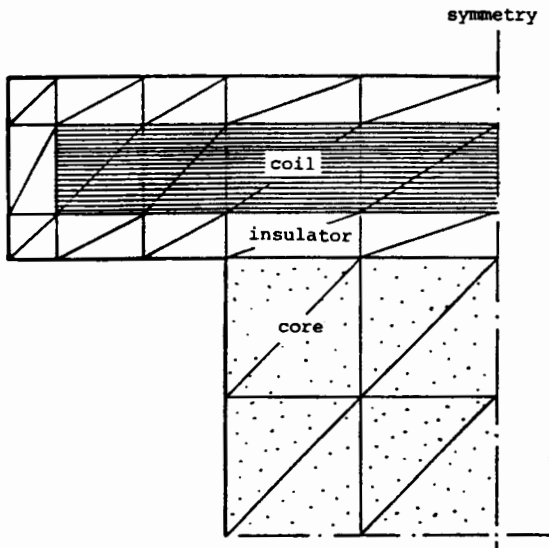
APPLICATION TO A DC-MACHINE ARMATURE

For comparison, we applied our method to the coils in the slots region covered by the insulation materials, the air holes in the armature core, and to the commutator region faced to the forced cooling air directly. The rating and dimensions of the tested motor are listed in Table 1. Table 2. shows the various conditions used for calculations. Also, various parameters of the experimental formula Eq. (4) are listed in the Table 3. The details of these formulae are described in Refs. [2,7,8].

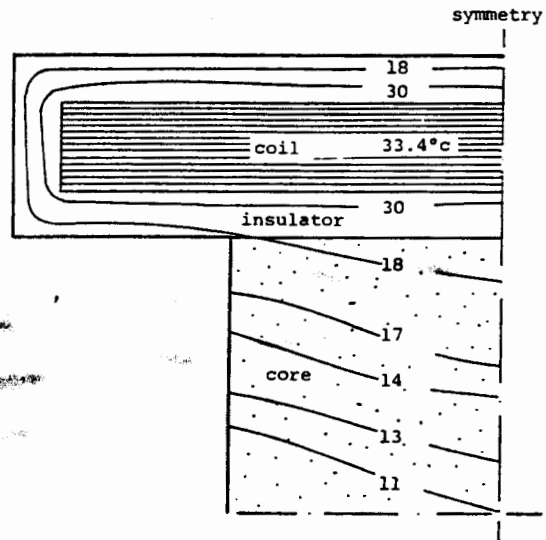
Fig. 3(a) shows the mesh system of the coil in the slots and coil end regions. Also, Fig. 3 (b) shows the mesh system of the commutator region. Fig. 4(a) and (b) show the calculated results. Furthermore, as shown in Fig. 5(a) and (b) the calculated results are compared with those of experimental ones.

Table 1. Rating and dimensions of the tested motor.

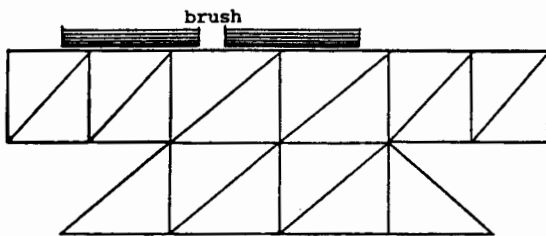
Rating			Dimension		
Output (Cont.)	[kW]	4.2	Diameter of the armature	[mm]	175
Rotating speed	[r.p.m.]	1350	Armature length	[mm]	150
Cooling air	[m ³ /min]	4.5	Diameter of the commutator	[mm]	120
Ventilating system	Forced air cooling		Commutator length	[mm]	65



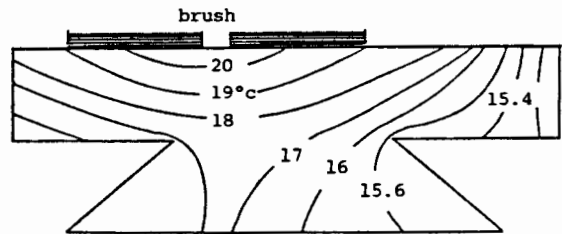
(a) Mesh system of coil in the slots, coil end, and core regions



(a) Coil in the slots, coil end, and core regions



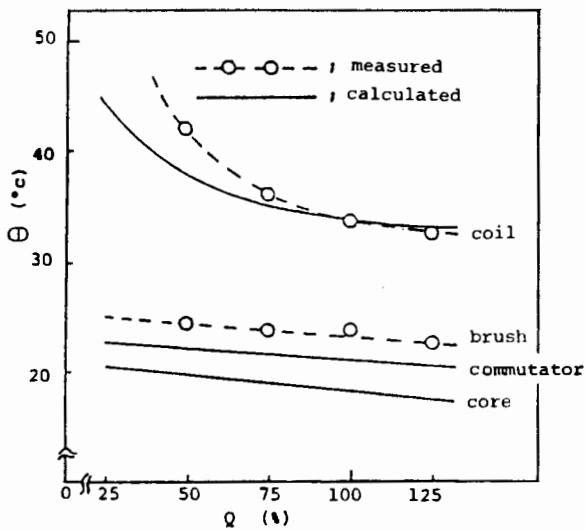
(b) Mesh system of commutator region



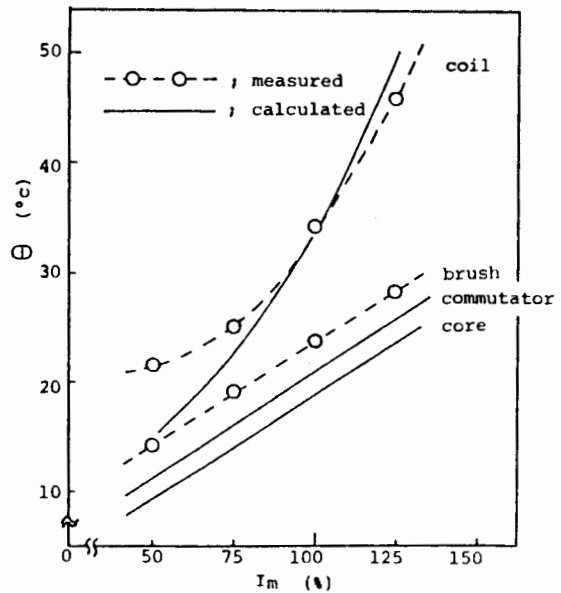
(b) Commutator region

Fig. 3. Triangular discretization of the regions.

Fig. 4. Calculated temperature rise distributions.



(a) Relationship between the temperature rise Θ and forced cooling air Q



(b) Relationship between the temperature rise Θ and motor current I_m

Fig. 5. Comparison of the calculated with experimented results of representative point.

Table 2. Various conditions used for calculations.

Heat source(Rating operation)	[W]	Thermal conductivity	[W/°c m]
Copper loss	250	Coil	381
No-load iron loss	100	Iron core	25
Brush electrical loss	100	Insulator	0.25
Commutator friction loss	80		

Table 3. Parameters used in each region.

- | |
|---|
| * coils in the slots region |
| a : radius of the armature |
| b : axial length of the armature core |
| c : gap length |
| * air holes in the armature core region |
| a : length of the air holes |
| b : diameter of the air holes |
| c : radius of the air hole centers |
| * commutator region |
| a : diameter of the commutator |
| b = c = 0 |

CONCLUSION

As shown above, we have tried to formulate the functionals taking into account the forced cooling condition. Even though our step is not mathematically rigorous, the results have revealed that our formulation promises the good results.

As the next step of our investigation, the authors plan to work out the calculation of transient temperature distribution of DC-machines armature.

REFERENCES

1. T. Yamamura and S. Yamazaki; J.I.E.E.J.86. 648, 1966.
2. S. Yamazaki and T. Yamamura; J.I.E.E.J.93. 493, 1973.
3. T. Yamamura, Y. Saito and H. Nakamura; Proceedings of ICEM, Part 2, HC 4, 1982.
4. T. Yamamura, S. Hayano, H. Inaba and Y. Saito; Annual meeting of IEEJ, No.835, 1977.
5. T. Yamamura, S. Hayano, H. Inaba and Y. Saito; Annual meeting of IEEJ, No. 842, 1977.
6. A. F. Armor and M. V. K. Chari; IEEE Trans. Power Apparatus and Systems, PAS-95, No.5, pp. 1643-1668, 1976.
7. S. Yamazaki and T. Yamamura; J.I.E.E.J. 92-B, 5, 287, 1972.
8. T. Yamamura and S. Yamazaki; J.I.M.E.J. 31, 427, 1965.